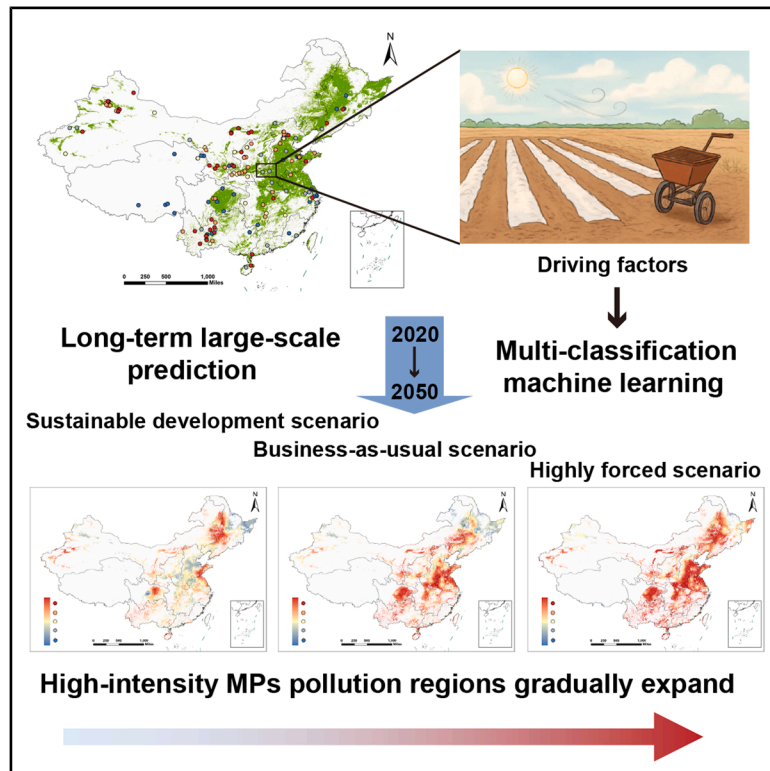


Microplastics pollution modulated by farming regimes under multi-scenarios

Graphical abstract



Authors

Xuan Li, Yajuan Shi, Xiangbo Xu, ..., Weixia Liu, Kexin Wei, Sinan Li

Correspondence

yajuanshi@rcees.ac.cn

In brief

Environmental science; Pollution;
Agricultural science

Highlights

- History of mulching films use as dominant driver of soil MPs pollution
- Identification of 0°C as tipping point for shifts in MPs abundance and size
- Soil MPs abundance may exceed 10,000 items/kg by 2050 under stress
- Sustainable development scenario shows slower growth of soil MPs pollution



Article

Microplastics pollution modulated by farming regimes under multi-scenarios

Xuan Li,^{1,2} Yajuan Shi,^{1,2,7,8,*} Xiangbo Xu,³ Qiran Zhao,⁴ Li Qian,^{1,2} Xiuqing Shao,^{1,2} Andrew C. Johnson,⁵ Xuan Zhou,^{1,2} Lianmian Shen,^{1,2} Weixia Liu,^{1,2} Kexin Wei,^{1,2} and Sinan Li^{1,6}

¹State Key Laboratory of Regional and Urban Ecology, Research Center for Eco-Environmental Sciences, Chinese Academy of Sciences, Beijing 100085, China

²University of Chinese Academy of Sciences, Beijing 100049, China

³Key Laboratory of Ecosystem Network Observation and Modeling, Institute of Geographic Sciences and Natural Resources Research, Chinese Academy of Sciences, Beijing 100101, China

⁴College of Economics and Management, China Agricultural University, Beijing 100083, China

⁵UK Centre for Ecology and Hydrology, Wallingford, OX10 8BB Oxfordshire, UK

⁶School of Ecology and Environmental Science, Yunnan University, Yunnan 650504, China

⁷Senior author

⁸Lead contact

*Correspondence: yajuanshi@rcees.ac.cn

<https://doi.org/10.1016/j.isci.2025.114208>

SUMMARY

With the growing challenge of microplastics (MPs) pollution, long-term real-time monitoring of MPs distribution remained difficult. Using nationwide field data and machine learning, we investigated MPs abundance and size distribution across China, key drivers, and future trends of MPs under multi-scenarios: sustainable development scenarios (SDSs), business-as-usual scenario (BAU), and high-forcing scenarios (HFSs). Results indicated that the average abundance of MPs in agricultural soils was 2,176 items/kg in 2020, with most particles smaller than 1 mm. The history of mulching film use (HistMF) was identified as the dominant factor influencing both MPs abundance and size, while climate variables such as radiation, temperature, and humidity further intensified fragmentation. Without intervention, MPs could exceed 10,000 items/kg by 2050 under the HFS. This research highlighted the need to strengthen mulching film production and plastic waste management in farmlands, particularly in regions with extreme climatic conditions, and provided scientific support for MPs control.

INTRODUCTION

Microplastics ([MPs] <5 mm) pollution has emerged as a disturbing global environmental challenge, affecting ecosystem functions, climate change, and environmental justice. MPs are largely formed by fragmentation of plastic waste in the environment under the effects of mechanical abrasion, weathering, and UV radiation.¹ Plastic waste accumulation in terrestrial environments has been predicted to exceed 10 billion tons, and without effective interventions, unrecycled and unmanaged plastic waste could reach 121 million tons annually by 2050.² Nevertheless, global efforts to tackle plastic pollution have made little progress. The recent INC-5 in Busan, South Korea, failed to reach a consensus on limiting total plastic production and the responsibility for plastic waste management, making the effective governance of MPs a difficult task.

Plastic mulching films significantly enhance productivity by increasing soil moisture and temperature and suppressing weed growth in agriculture. However, residual mulching films, which are difficult to recycle, gradually degrade into MPs over time, potentially leading to a decline in soil quality and causing physiolog-

ical and biochemical harm to biological communities and potential bioaccumulation in higher trophic levels.^{3–5} MPs can serve as vectors, carrying pollutants such as pesticides, heavy metals, and antibiotics, thereby causing additional harm to organisms and human health.⁶ The size of MPs is a key factor influencing their toxicity. For instance, research has demonstrated that the roots of wheat and lettuce can absorb polystyrene particles as small as 2 μm .⁷ It has been shown that earthworms can selectively ingest MPs, preferring those with smaller particle size (especially smaller than 50 μm).⁸ Hence, in the context influenced by human activities and climate change, it is crucial to consider the formation, abundance, and size of MPs in agricultural soils. Such studies are essential to provide scientific evidence for agricultural ecological safety and sustainable development.

Systematic quantification of MPs in soils began only in the past decade, with existing research primarily focused on small-scale or specific farmlands, leaving current data relatively limited.⁹ Large-scale and multi-temporal sampling and analysis of MPs demand significant human, temporal, and financial resources.^{10,11} Some experiments have simulated mechanical abrasion and UV radiation to calculate the emission factor (EF)



of plastic film fragmentation into MPs and to estimate MPs emissions resulting from mulching films in agricultural soils.¹² These MPs quantification models from these short-term controlled experiments are often restricted to single variables and sources. However, the long-term accumulation of MPs in real-world environments involves multiple variables and sources, such as mechanical abrasion, radiation, mulching films, and organic fertilizers, which are not fully reflected in current models. Machine learning (ML) has increasingly emerged as a powerful tool to automatically learn and extract complex patterns from data and capture nonlinear relationships.¹³ Research has demonstrated that ML approaches offer advantages in utilizing existing databases to predict the polymer types and biological hazards associated with MPs.¹⁴ Here, we extend this approach to analyze driving factors and existing data, enabling large-scale, multi-temporal data expansion and predictions of MPs abundance and size distribution.

China, as a major country in agricultural production and plastic waste generation, with its diverse terrain, climate, and agricultural practices, represents an ideal region for exploring large-scale MPs pollution and its driving factors. This study involved several stages. First was the collection of data on MPs abundance and size in agricultural soils across China from published literature. Second, the analysis focused on the driving factors that influence their distribution, including the history of mulching film use (HistMF), usage of mulching films (UMF), usage of organic fertilizers (UOF), and climatic factors such as temperature (TEM), humidity (HUM), radiation (RAD), and wind speed (WS), as well as topographic factors like slope (SL) and elevation (ELE). Third was the development of multi-classification ML models to achieve two objectives: (1) simulating the spatial distribution of MPs abundance and size in current agricultural soils and identifying their key driving factors and (2) analyzing dynamic factors, such as policy interventions and climate change, to predict the spatial distribution and temporal evolution trends of MPs under multi-scenarios.

RESULTS AND DISCUSSION

Reported microplastics data in agricultural soils across China

Data available on field investigations of MPs are very uneven globally.¹⁵ Asia was estimated to be the largest user of plastics in agricultural production, accounting for almost half of the global usage.¹⁶ China is the country that has performed the most MPs measurements according to our quantitative analysis, covering all agricultural regions. Agricultural land was divided into nine agricultural regions according to the comprehensive agricultural regionalization of the country due to climatic conditions, geographical locations, and cropping systems varying significantly across China. The levels of MPs in agricultural soils in China are globally representative, with an average abundance of $4,892 \pm 558$ items/kg, comparable to the soils used for plastic-mulched crops in the United Kingdom ($4,689 \pm 147$ items/kg).¹⁷ The average MPs abundance in the Huang-Huai-Hai Plain region aligns closely with Chilean agricultural soils, reported at 540 items/kg.¹⁸ Meanwhile, the levels of MPs in the Qinghai-Tibet Plateau region are similar to German agricultural topsoil,

measured at 15.8 items/kg (Figures 1A and 1B).¹⁹ The average size of MPs in agricultural soils is 827 ± 44 μm , with 60% of the sampling sites containing MPs smaller than 1 mm (Figures 1C and 1D), indicating the prevalence of smaller-sized MPs in the soil.¹⁰ The abundance of MPs in agricultural soils across China varies greatly, ranging from a few to tens of thousands of items per kilogram. This wide variation underscores the necessity for a broad assessment of driving factors behind the MP contamination in agricultural environments.

An ordered classification of MPs abundance and size

A descriptive analysis of the reported MPs abundance data from published literature revealed that it follows a log-normal distribution. We divided the MPs abundance data into five equal segments and found that the cutoff points were approximately at 500, 1,500, 3,000, and 6,000 items/kg (Table S1). Therefore, we categorized MPs abundance into five classifications: <500, 500–1,500, 1,500–3,000, 3,000–6,000, and >6,000 items/kg, enabling the accurate and rapid determination of MPs levels in a given region (Figure 1B). For instance, MPs abundance was reported to range from 3 to 210 items/kg in Hebei province, China, corresponding to the lowest level I.²⁰ The abundance of MPs ranged from 310 to 5,698 items/kg in Shouguang, Shandong Province, falling within levels II, III, and IV.²¹ Additionally, it has been reported that the average MPs abundance in five northern provinces of China (Gansu, Shanxi, Hebei, Shaanxi, and Inner Mongolia) was 14,629, 10,811, 10,756, 9,550, and 9,500 items/kg, respectively, corresponding to the highest level V.²²

The classification of MPs size is based on established standards, where MPs between 1 and 5 mm are defined as large-sized MPs and those smaller than 1 mm are categorized as small-sized MPs.²³ Reports indicate that the majority of MPs in soils are smaller than 1,000 μm .²¹ For the further classification of small MPs, we divided the natural logarithm (Ln) of the MP size data into five equal segments, which revealed that the size cutoffs were approximately at 200, 500, 1,000, and 1,500 μm (Table S1). Based on this division, we then determined the specific size ranges, which are 10–200, 200–500, 500–1,000, 1,000–1,500, and 1,500–5,000 μm (Figure 1D). An ordered classification of soil MPs pollution in terms of both abundance and size is presented, with a uniform distribution of sampling points across each classification range on a national scale, providing a robust basis for categorization.

Interpretation of factors—based on machine learning

The XGBoost multi-classification model demonstrated a strong predictive ability with an accuracy of 0.717 for predicting MPs abundance (Figure S1; Table S2). We conducted a comprehensive analysis of the effects of each factor and the interaction factors on MPs abundance and size. The results indicated that most driving factors had a complex and nonlinear impact on MPs abundance. However, HistMF exhibited a consistent and linear relationship with MPs abundance, particularly when HistMF reached 15 years, where MPs abundance significantly increased (Figures 2A and S2A). A survey of mulching films and MPs across 41 households in Hebei Province revealed a positive correlation between HistMF and MPs abundance.²⁰ The interaction between HistMF and RAD showed a significant synergistic effect

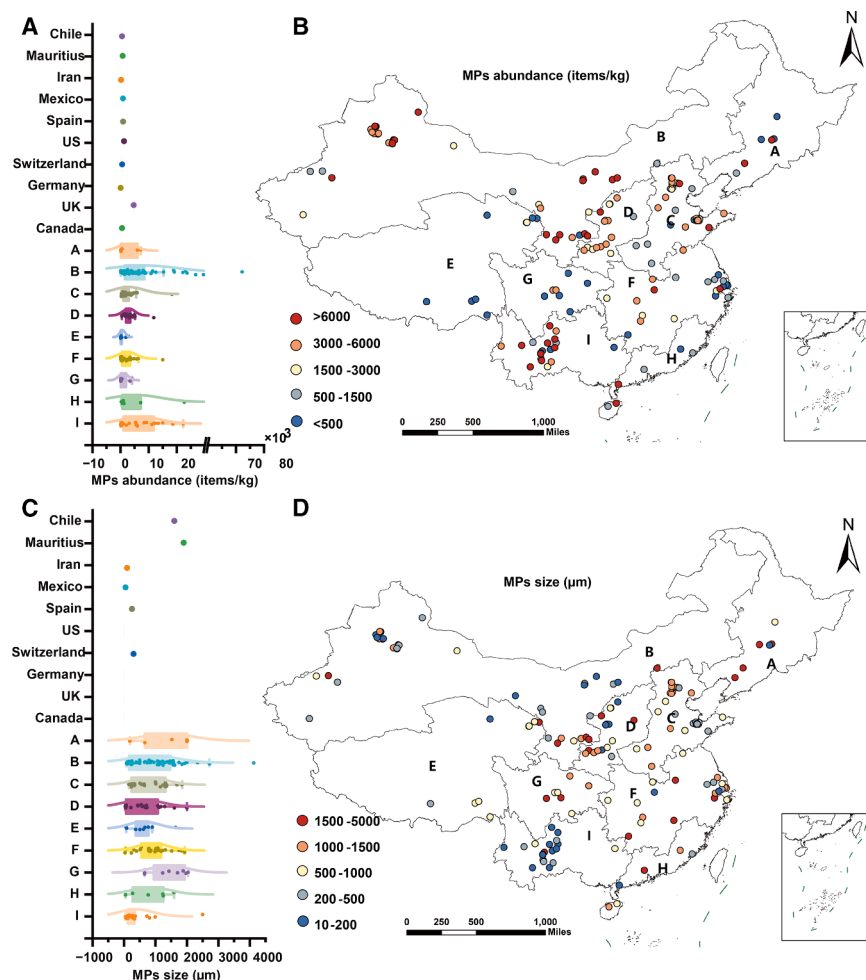


Figure 1. Comparisons of MPs abundance and size across different regions of China and selected international datasets

MPs abundance (A) and size (C) in China and representative values for the other countries from published literature. MPs abundance (B) and MPs size (D) in nine agricultural regions of China. The nine agricultural regions are A. Northeast China Plain, B. northern arid and semiarid region, C. Huang-Huai-Hai Plain, D. Loess Plateau, E. Qinghai Tibet Plateau, F. Middle-lower Yangtze Plain, G. Sichuan Basin and surrounding regions, H. Southern China, and I. Yunnan-Guizhou Plateau.

in areas with gentler slope and intensive agricultural activity.^{26,27} The results revealed that the relationship between ELE and MP abundance is complex and influenced by other factors. The interaction between HistMF and WS on MPs abundance exhibited a phenomenon of rapid increase and rapid decrease (Figure 2F). This phenomenon was attributed to the generation of surface shear stress, which triggered soil wind erosion and the entry of soil MPs into the atmosphere,²⁸ yet still resulted in a higher MPs abundance compared to lower WS.

The XGBoost model performed well in predicting MPs size, with an accuracy of 0.652 (Figure S1; Table S2). The results showed that the extension of HistMF led to a general reduction in MPs size, especially when HistMF was 15 years, where

on MPs abundance (Figures 2D and S2C), especially when the HistMF exceeded 20 years and RAD intensity reached 6,000 MJ/year (Figure 2B), causing a sharp increase in MPs abundance. Previous studies suggested that with increasing RAD intensity, when RAD intensity increased from 1,642 to 2,632 MJ/m², the EF of PE films rose from 2.80 to 8.43 mg/g.¹² MPs abundance was higher at lower TEM (<5°C), and as the TEM increased, the abundance quickly decreased (Figure 2C), which may have been due to MPs being more prone to fragmentation at low temperatures. Additionally, in regions with lower temperatures, agricultural crops were highly dependent on plastic films. Moreover, as the TEM rose above 20°C, MPs abundance increased and a synergistic effect was observed with HistMF (Figure 2E).

TEM and ELE showed a synergistic effect (Figure S2C), where the higher RAD accompanying higher ELE accelerated the degradation and fragmentation of residual plastic films, leading to more MPs being released. In the Qinghai-Tibetan Plateau, the abundance of MPs in agricultural soils above 2,000 m is significantly higher than at 1,000 m.²⁴ Except for radiation erosion, areas with melting snow and ice can release MPs.²⁵ However, another research revealed a negative correlation between MPs abundance and ELE, which is likely due to MPs accumulation

the size remained small (Figure 2G). However, as HistMF extended beyond 20 years, MPs size increased, which was due to the lower degree of plastic film fragmentation in regions like Xinjiang and Gansu. With increasing UOF, the size of MPs gradually decreased (Figure 2H). Multiple studies had shown that MPs in organic fertilizers originated from plastic mulching, animal feed, and food waste, and MPs size further decreased during processing, with smaller MPs accounting for a large proportion.^{29,30} Additionally, TEM, HUM, the interaction between TEM and HUM, and the interaction between HistMF and TEM all exhibited a pattern of first increasing and then decreasing (Figures 2I, 2J, 2K, and S2D), indicating that MPs size tended to decrease under too dry or high-humidity and too low- or high-temperature conditions. TEM fluctuations induce the contraction and expansion of plastics, releasing smaller MPs. Rising TEM increases the frequency of extreme weather events, which may cause droughts that trap MPs in the soil.^{31,32} The interaction between high HUM and RAD synergistically increases MPs abundance (Figure 2L). Previous research has shown that UV exposure causes chemical bond dissociation in polypropylene plastics, leading to fragmentation into MPs, particularly in surface soils.³³ More abundant MPs with small size were found in the higher altitudes than low ones in the Qinghai-Tibetan

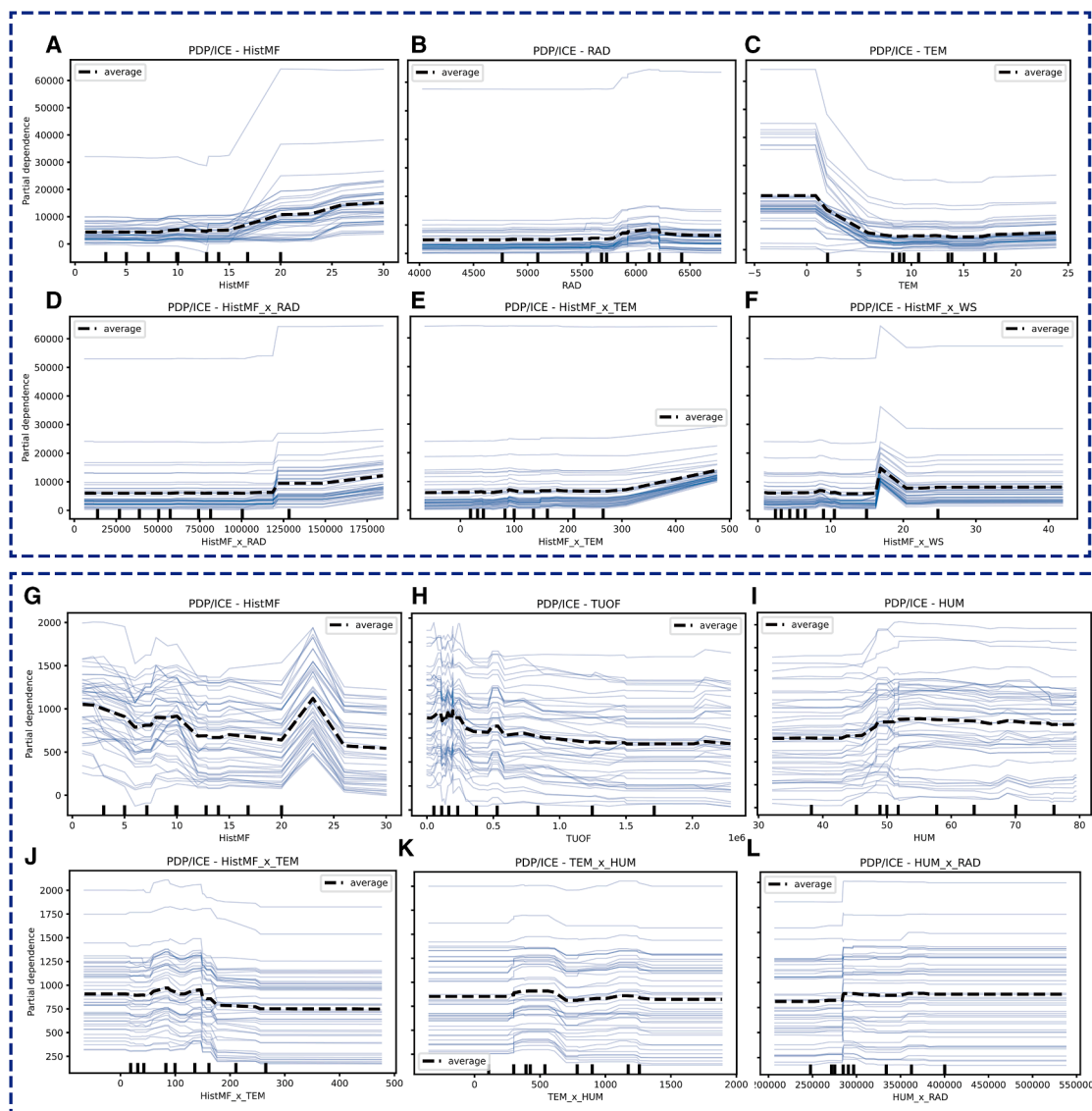


Figure 2. Relationship of MPs abundance and size with driving and interacting features

Partial dependence plots (PDP) and individual conditional expectation (ICE) plots for the driving and interacting features of MPs abundance (A–F) and size (G–L). The black dashed line indicates the average prediction (PDP), while the light blue lines show the individual ICE curves for each observation. The x axis represents the feature values, and the y axis shows the model predicted response (MPs abundance or size).

Plateau.²⁴ This can be attributed to intense UV radiation at high ELE, which accelerates the photodegradation and aging of plastics.³⁴ This suggested that the synergistic effect of environmental factors played an important role in the changes in the physical properties of MPs.

Extension of MPs abundance and size data in 2020

The abundance and size of MPs in agricultural soils across China were simulated and expanded using an XGBoost multiclassification model, which extended the scattered MPs data to achieve full spatial and finer coverage of MPs data. The average abundance of MPs in 2020 of agricultural soils across China was $2,176 \pm 227$ items/kg, with 3.51% of croplands showing abun-

dance exceeding 6,000 items/kg (Figure 3A), which aligns closely with the nationwide MPs abundance ($2,462 \pm 3,767$ items/kg) based on 477 samples.³⁵ Among the nine agricultural regions, the northern arid and semiarid region exhibited the highest MPs abundance (3,871 items/kg) (Figure 3B), which is associated with the extensive UMF and the rapid degradation of residues under dry climatic conditions. Agricultural regions along the eastern coast and in central areas, as core regions for agricultural production,³⁶ exhibit relatively high abundance, and the accumulation of MPs over long-term agricultural practices adversely affects soil structure and crop growth. Particularly noteworthy is the Qinghai-Tibet Plateau, which has the lowest MPs abundance (803 items/kg). Despite these low values, the

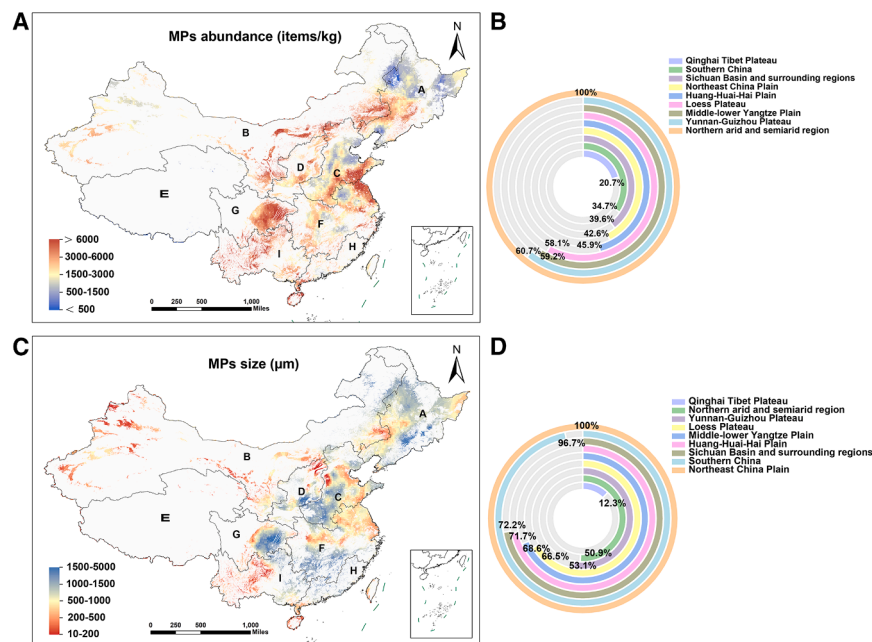


Figure 3. Simulation extension of MPs abundance and size in agricultural soil of China

Heatmap and comparison of MPs abundance (A and B) and size (C and D) in 2020 across the nine major agricultural regions. Areas with color bands closer to red indicate higher abundance and smaller size of MPs, while areas closer to blue indicate lower abundance and larger size.

nario of worsening pollution, with MPs abundance reaching $10,465 \pm 1,219$ items/kg by 2050, significantly exceeding the BAU level of $7,844 \pm 989$ items/kg. In contrast, under the SDS, MPs abundance is reduced to $4,716 \pm 265$ items/kg by 2050, representing only 60% of the BAU (Figure 4A). The proportion of MPs abundance in different categories shows that under SDS, the 1,500–3,000 items/kg range dominates. In contrast, under BAU and HFS, areas exceeding 6,000 items/kg are most prevalent (Figure 4B).

plateau's unique high-altitude, cold climate, and rapid degradation processes contribute to the strong diffusivity of MPs, which may spread through natural forces like wind.²⁶ Long-term exposure could have a lasting impact on the ecosystem in this sensitive region. Therefore, monitoring and management of MPs in the Qinghai-Tibet Plateau should also be prioritized to prevent potential ecological threats.

MPs size distribution showed that 61% of MPs croplands had a particle size of $<1,000 \mu\text{m}$ (Figure 3C). The average MPs size in the Northeast Plain is the largest, reaching $1,054.21 \mu\text{m}$, which may be attributed to the moderate climate conditions leading to slower degradation, whereas the Qinghai-Tibet Plateau exhibited the smallest average size ($129.46 \mu\text{m}$) (Figure 3D), possibly due to accelerated degradation caused by intense radiation and the input of small-sized MPs from organic fertilizers. MPs in the northern arid and semiarid regions, Huang-Huai-Hai Plain, and Yunnan-Guizhou Plateau exhibit high abundance (2,249–3,871 items/kg) and relatively smaller size (536.96 – $756.26 \mu\text{m}$), as shown in the red spectrum of the heatmap (Figure 3). MPs in these regions have increased diffusivity, smaller particles more likely to spread through water and soil,^{37,38} potentially threatening water sources and the environment, thus requiring prioritized monitoring and management.

Projected distribution of MPs under multi-scenarios

MPs abundance is predicted to show a continuous upward trend across all scenarios until 2040. Under the sustainable development scenario (SDS), the growth rate of MPs abundance is the slowest, increasing by 1.62 times compared to 2020 ($2,176 \pm 227$ items/kg). In contrast, the business-as-usual scenario (BAU) and the high-forcing scenario (HFS) show sustained increases, with growth rates of 2.98 times and 3.98 times, respectively. MPs abundance declines under the SDS and BAU, while it continues to rise under HFS by 2050 (Figure 4A). The HFS reflects a sce-

Heatmap analysis shows that as climate scenarios worsen and the UMF increases, high-concentration regions (darker areas) gradually expand (Figures 4C–4E). In the three assumed scenarios, changes in plastic film residue are represented by a 10% annual reduction of UMF in SDS and a 10% annual increase in HFS. Empirical evidence shows that within 1 m of plastic residue hotspots, MPs abundance can reach as high as 75,000 items/kg, suggesting that the presence of plastic residues markedly elevates MPs levels in adjacent soils.^{39,40} Under different future socioeconomic pathways, climate drivers exhibit pronounced divergence. Regarding TEM, both global and regional means in China are projected to increase under SSP1-2.6 (SDS), SSP2-4.5 (BAU), and SSP5-8.5 (HFS), with stronger warming associated with more intensive emission scenarios. The SSP5-8.5 pathway produces the most pronounced warming, accompanied by a substantial rise in the frequency and intensity of extreme heat events.^{41,42} Likewise, extreme humid-heat conditions are projected to deteriorate considerably under HFS.⁴³ Changes in RAD and WS are comparatively weaker but exhibit significant regional variability, with an amplified trend observed over mid-latitude continental regions.^{44,45} In line with earlier analyses linking explanatory variables to MPs abundance, both TEM and RAD display synergistic effects with the HistMF, significantly amplifying MPs accumulation. Over time, plastic residues undergo weathering and fragment into smaller particles.⁴⁶ Plastic films are particularly vulnerable to solar radiation and oxidative processes, which promote photo-oxidative degradation.³³ Likewise, the major sources of model uncertainty can be attributed to HistMF, TEM, RAD, and HUM (Figure S3). Collectively, the trajectory of MPs abundance is jointly driven by accelerating climate change and inadequate plastic waste management.

MPs size consistently exhibits a distinct normal distribution, with the majority falling within the mid-range category of

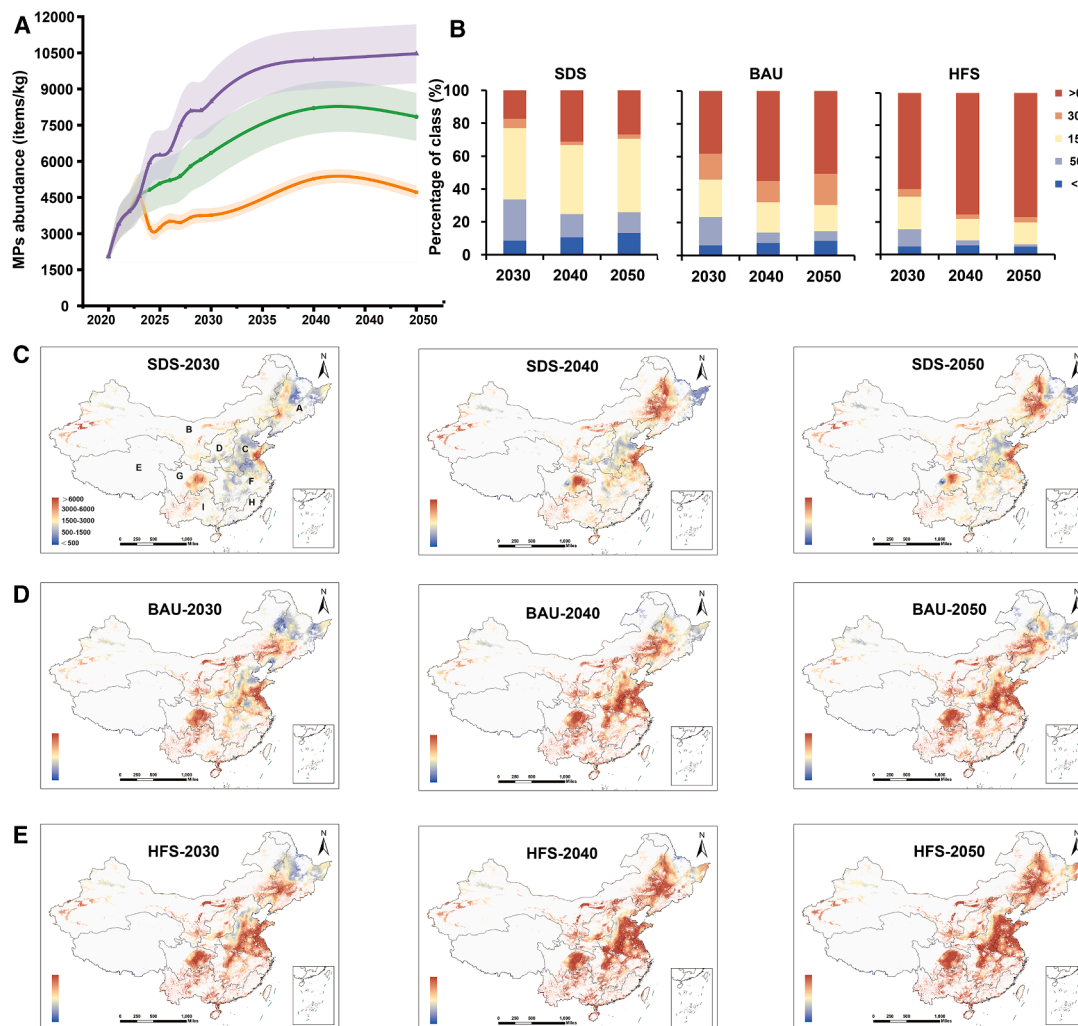


Figure 4. Forecast of MPs abundance to 2050

Nationwide average MPs abundance over time, with supplementary simulations for 2020–2023 and future scenario predictions for 2024–2050 (A). The proportion of MPs abundance at different categories under SDS, BAU, and HFS in 2030, 2040, and 2050 (B). Heatmaps of MPs abundance under SDS (C), BAU (D), and HFS (E) in 2030, 2040, and 2050. Areas with color bands closer to red indicate higher abundance, while areas closer to blue indicate lower abundance.

500–1,000 μm , while larger and smaller sizes are less frequent (Figures 5A and 5B). Under SDS, most MPs size concentrated in the 500–1,000 μm range (Figure 5C). However, under BAU and HFS, the proportion of MPs size <500 μm increases, particularly in northern arid/semi-arid regions, the Huang-Huai-Hai Plain, and the Yunnan-Guizhou Plateau (Figures 5D and 5E). Manure-based fertilizers are widely used in these regions, primarily to enhance soil fertility and improve crop quality. However, the application of these fertilizers can inadvertently contribute to MPs pollution. During aerobic composting, plastic waste in organic fertilizers undergoes intense free radical reactions, resulting in fragmentation and a significant increase in the number of MPs.^{47,48} Anaerobic digestion further causes embrittlement and fragmentation of plastics, while mechanical processes in fertilizer production, including crushing, granulation, drying, cooling, and screening, can also contribute to the breakdown of plastics into smaller MPs.⁴⁹ Global climate change indicates

that humidity in wet regions may further increase, while arid regions are expected to become drier. Additionally, arid climates may drive higher demand for mulching films. This trend of climatic “polarization” has significant implications for MPs pollution, as the increased UMF under arid conditions, coupled with inadequate recycling practices, lead to higher abundance and smaller size. Although the exact mechanisms of how MPs size affects biological toxicity remain somewhat controversial, size is a key factor influencing toxicity.⁵⁰ Researches have shown that smaller MPs are more easily ingested by organisms.⁵¹ Therefore, determining the MPs size in soil is a necessary step for conducting ecological risk assessments.

Conclusions and implications

Based on nationwide field data and ML simulations, this research systematically revealed the evolution trends of agricultural soil MPs under various future scenarios. The results

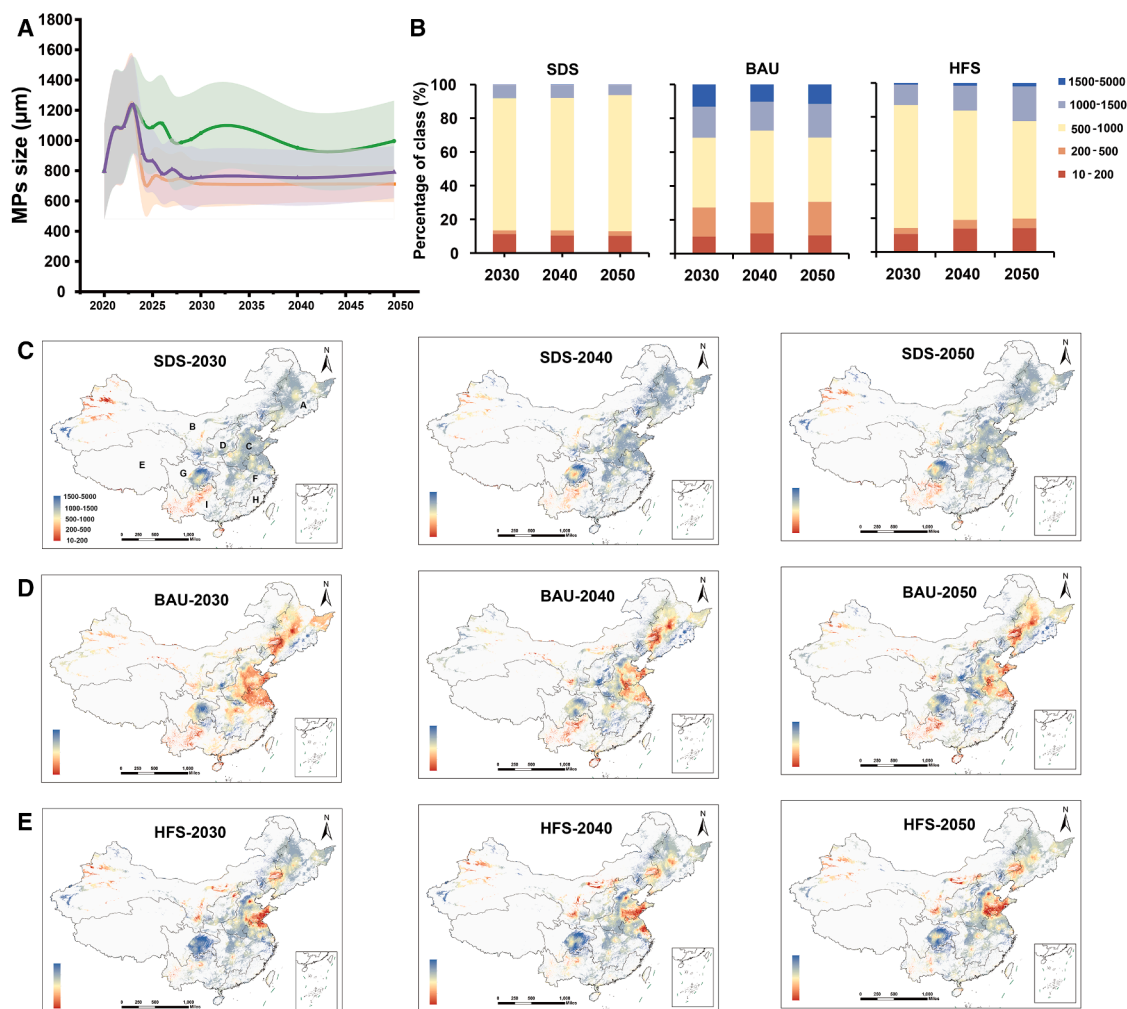


Figure 5. Forecast of MPs size to 2050

Nationwide average MPs size over time, with supplementary simulations for 2020–2023 and future scenario predictions for 2024–2050 (A). The proportion of MPs size at different categories under SDS, BAU, and HFS in 2030, 2040, and 2050 (B). Heatmaps of MPs size under SDS (C), BAU (D), and HFS (E) in 2030, 2040, and 2050. Areas with color bands closer to red indicate smaller size of MPs, while areas closer to blue indicate larger size.

indicated that, without effective interventions, the abundance of MPs in China's agricultural soils might increase nearly five times by 2050 under HFS, with an average concentration exceeding 10,000 items/kg. In the SDS, however, the abundance was only 4,716 items/kg, approximately 60% of the BAU scenario, suggesting that strengthening agricultural film management and emission reduction measures could significantly mitigate the expansion of pollution. The model also accurately predicted that most MPs size in agricultural soils were $<1,000$ μm . Furthermore, the model revealed that HistMF was the key factor determining MPs abundance and size, with significant interactions with climate variables such as RAD, TEM, and HUM, which further amplified the risk of MPs accumulation. These results provided quantitative evidence for the effectiveness of related policies.

Based on these findings, we recommend strengthening the quality supervision of mulching film production and encouraging

the use of standard-thickness or biodegradable films in regions with high radiation, distinct wet-dry seasons, or long HistMF, in combination with policy subsidies to alleviate farmers' economic burdens. Additionally, we suggested that MPs should be incorporated as a monitoring indicator in the organic fertilizer production process to reduce input sources, and that unified MPs monitoring standards and techniques should be adopted in the future to ensure data comparability and consistency.

Limitations of the study

The limitation of this study lay primarily in its reflection of macro-scale patterns rather than site-specific or crop-level processes. Highly heterogeneous variables such as crop types were intentionally excluded to maintain model stability and data consistency. Although the data for China were relatively comprehensive, there were gaps in spatial coverage and regional disparities, and key indicators such as agricultural film recycling

rates had not been disclosed, leading to uncertainty in distribution assessments. Future research should incorporate finer-scale variables, such as crop types and soil properties, and conduct long-term systematic monitoring across diverse climate zones to enhance the generalizability and external validity of the conclusions.

RESOURCE AVAILABILITY

Lead contact

Requests for further information and resources should be directed to and will be fulfilled by the lead contact, Yajuan Shi (yajuanshi@rcees.ac.cn).

Materials availability

This study did not generate new unique reagents.

Data and code availability

- Data: All data reported in this paper will be shared by the [lead contact](#) upon request.
- Code: This article does not report original code.
- Additional information: Any additional information required to reanalyze the data reported in this article is available from the [lead contact](#) upon request.

ACKNOWLEDGMENTS

This work was financially supported by the National Key R&D Program of China (2023YFC3705902 and 2023YFC3804902) and China Postdoctoral Science Foundation (2024M753419).

AUTHOR CONTRIBUTIONS

Conceptualization, Y.S., X.X., and Q.Z.; methodology, Y.S., X.X., and X.L.; software, L.Q. and X.Z.; investigation, A.C.J., L.S., and W.L.; writing – original draft, X.L.; writing – review and editing, Y.S., and A.C.J.; visualization, X.L., K.W., and S.L.; supervision, Y.S. and X.X.; funding acquisition, Y.S. and L.Q.

DECLARATION OF INTERESTS

The authors declare no competing interests.

STAR★METHODS

Detailed methods are provided in the online version of this paper and include the following:

- [KEY RESOURCES TABLE](#)
- [METHOD DETAILS](#)
 - Collection of MPs data in agricultural soils
 - Data standardization and legitimacy of integrated analysis
 - Analysis and collection of factors
 - Data preprocessing and machine learning modeling
 - Future scenario construction
 - Expansion and prediction of MPs distribution
 - Uncertainty analysis
- [QUANTIFICATION AND STATISTICAL ANALYSIS](#)

SUPPLEMENTAL INFORMATION

Supplemental information can be found online at <https://doi.org/10.1016/j.isci.2025.114208>.

Received: July 4, 2025

Revised: October 9, 2025

Accepted: November 20, 2025

Published: November 25, 2025

REFERENCES

1. Lozano, Y.M., and Rillig, M.C. (2020). Effects of microplastic fibers and drought on plant communities. *Environ. Sci. Technol.* 54, 6166–6173. <https://doi.org/10.1021/acs.est.0c01051>.
2. Pottinger, A.S., Geyer, R., Biyani, N., Martinez, C.C., Nathan, N., Morse, M.R., Liu, C., Hu, S., de Bruyn, M., Boettiger, C., et al. (2024). Pathways to reduce global plastic waste mismanagement and greenhouse gas emissions by 2050. *Science* 386, 1168–1173. <https://doi.org/10.1126/science.adr3837>.
3. Li, L., Luo, Y., Li, R., Zhou, Q., Peijnenburg, W.J.G.M., Yin, N., Yang, J., Tu, C., and Zhang, Y. (2020). Effective uptake of submicrometre plastics by crop plants via a crack-entry mode. *Nat. Sustain.* 3, 929–937. <https://doi.org/10.1038/s41893-020-0567-9>.
4. Sun, X.D., Yuan, X.Z., Jia, Y., Feng, L.J., Zhu, F.P., Dong, S.S., Liu, J., Kong, X., Tian, H., Duan, J.L., et al. (2020). Differentially charged nanoplastics demonstrate distinct accumulation in *Arabidopsis thaliana*. *Nat. Nanotechnol.* 15, 755–760. <https://doi.org/10.1038/s41565-020-0707-4>.
5. Kumar, M., Xiong, X., He, M., Tsang, D.C.W., Gupta, J., Khan, E., Harrad, S., Hou, D., Ok, Y.S., and Bolan, N.S. (2020). Microplastics as pollutants in agricultural soils. *Environ. Pollut.* 265, 114980. <https://doi.org/10.1016/j.envpol.2020.114980>.
6. Osman, A.I., Hosny, M., Eltaweil, A.S., Omar, S., Elgarahy, A.M., Farghali, M., Yap, P.S., Wu, Y.S., Nagandran, S., Batumalaie, K., et al. (2023). Microplastic sources, formation, toxicity and remediation: a review. *Environ. Chem. Lett.* 21, 1–41. <https://doi.org/10.1007/s10311-023-01593-3>.
7. Li, L., Luo, Y., Li, R., Zhou, Q., Peijnenburg, W.J.G.M., Yin, N., Yang, J., Tu, C., and Zhang, Y. (2020). Effective uptake of submicrometre plastics by crop plants via a crack-entry mode. *Nat. Sustain.* 3, 929–937. <https://doi.org/10.1038/s41893-020-0567-9>.
8. Cui, W., Gao, P., Zhang, M., Wang, L., Sun, H., and Liu, C. (2022). Adverse effects of microplastics on earthworms: A critical review. *Sci. Total Environ.* 850, 158041. <https://doi.org/10.1016/j.scitotenv.2022.158041>.
9. Liu, M., Lu, S., Song, Y., Lei, L., Hu, J., Lv, W., Zhou, W., Cao, C., Shi, H., Yang, X., et al. (2018). Microplastic and mesoplastic pollution in farmland soils in suburbs of Shanghai, China. *Environ. Pollut.* 242, 855–862. <https://doi.org/10.1016/j.envpol.2018.07.051>.
10. Hu, J., He, D., Zhang, X., Li, X., Chen, Y., Wei, G., Zhang, Y., Ok, Y.S., and Luo, Y. (2022). National-scale distribution of micro(meso)plastics in farmland soils across China: Implications for environmental impacts. *J. Hazard. Mater.* 424, 127283. <https://doi.org/10.1016/j.jhazmat.2021.127283>.
11. Harrison, S. (2023). Predicting the fate of plastic in the environment. *Nat. Water* 1, 490–491. <https://doi.org/10.1038/s44221-023-00097-2>.
12. Ren, S.Y., and Ni, H.G. (2022). A method for measuring the emissions of in situ agricultural plastic film microplastics by ultraviolet and mechanical abrasion. *Sci. Total Environ.* 819, 152041. <https://doi.org/10.1016/j.scitotenv.2021.152041>.
13. Zhong, S., Zhang, K., Bagheri, M., Burken, J.G., Gu, A., Li, B., Ma, X., Marone, B.L., Ren, Z.J., Schrier, J., et al. (2021). Machine Learning: New Ideas and Tools in Environmental Science and Engineering. *Environ. Sci. Technol.* 55, 12741–12754. <https://doi.org/10.1021/acs.est.1c01339>.
14. Yu, F., and Hu, X. (2022). Machine learning may accelerate the recognition and control of microplastic pollution: Future prospects. *J. Hazard. Mater.* 432, 128730. <https://doi.org/10.1016/j.jhazmat.2022.128730>.
15. Büks, F., and Kaupenjohann, M. (2020). Global concentrations of microplastic in soils, a review. *Soil* 2020, 1–26. <https://doi.org/10.5194/soil-6-649-2020>.
16. FAO (2021). Plastics in agri-food systems: The good, the bad, and the ugly. <https://www.fao.org/newsroom/detail/plastics-in-agrifood-systems-the-good-the-bad-and-the-ugly/en>.
17. Cusworth, S.J., Davies, W.J., McAinsh, M.R., and Stevens, C.J. (2024). A nationwide assessment of microplastic abundance in agricultural soils:

- The influence of plastic crop covers within the United Kingdom. *Plants People Planet* 6, 304–314. <https://doi.org/10.1002/ppp3.10430>.
18. Corradini, F., Casado, F., Leiva, V., Huerta-Lwanga, E., and Geissen, V. (2021). Microplastics occurrence and frequency in soils under different land uses on a regional scale. *Sci. Total Environ.* 752, 141917. <https://doi.org/10.1016/j.scitotenv.2020.141917>.
 19. Harms, I.K., Diekötter, T., Troegel, S., and Lenz, M. (2021). Amount, distribution and composition of large microplastics in typical agricultural soils in Northern Germany. *Sci. Total Environ.* 758, 143615. <https://doi.org/10.1016/j.scitotenv.2020.143615>.
 20. Xu, L., Xu, X., Li, C., Li, J., Sun, M., and Zhang, L. (2022). Is mulch film itself the primary source of meso- and microplastics in the mulching cultivated soil? A preliminary field study with econometric methods. *Environ. Pollut.* 299, 118915. <https://doi.org/10.1016/j.envpol.2022.118915>.
 21. Yu, L., Zhang, J., Liu, Y., Chen, L., Tao, S., and Liu, W. (2021). Distribution characteristics of microplastics in agricultural soils from the largest vegetable production base in China. *Sci. Total Environ.* 756, 143860. <https://doi.org/10.1016/j.scitotenv.2020.143860>.
 22. La, Y., Zhang, L., Zhao, N., Ye, H., Zeng, Q., Zhao, L., Wang, Z., Lin, D., and Wang, R. (2024). The microplastics distribution characteristics and their impact on soil physicochemical properties and bacterial communities in food legumes farmland in northern China. *J. Hazard. Mater.* 471, 134282. <https://doi.org/10.1016/j.jhazmat.2024.134282>.
 23. Eerkes-Medrano, D., Thompson, R.C., and Aldridge, D.C. (2015). Microplastics in freshwater systems: a review of the emerging threats, identification of knowledge gaps and prioritisation of research needs. *Water Res.* 75, 63–82. <https://doi.org/10.1016/j.watres.2015.02.012>.
 24. Feng, S., Lu, H., Yao, T., Xue, Y., Yin, C., and Tang, M. (2021). Spatial characteristics of microplastics in the high-altitude area on the Tibetan Plateau. *J. Hazard. Mater.* 417, 126034. <https://doi.org/10.1016/j.jhazmat.2021.126034>.
 25. Dong, H., Wang, L., Wang, X., Xu, L., Chen, M., Gong, P., and Wang, C. (2021). Microplastics in a Remote Lake Basin of the Tibetan Plateau: Impacts of Atmospheric Transport and Glacial Melting. *Environ. Sci. Technol.* 55, 12951–12960. <https://doi.org/10.1021/acs.est.1c03227>.
 26. Feng, S., Lu, H., and Liu, Y. (2021). The occurrence of microplastics in farmland and grassland soils in the Qinghai-Tibet plateau: Different land use and mulching time in facility agriculture. *Environ. Pollut.* 279, 116939. <https://doi.org/10.1016/j.envpol.2021.116939>.
 27. Lang, M., Wang, G., Yang, Y., Zhu, W., Zhang, Y., Ouyang, Z., and Guo, X. (2022). The occurrence and effect of altitude on microplastics distribution in agricultural soils of Qinghai Province, northwest China. *Sci. Total Environ.* 810, 152174. <https://doi.org/10.1016/j.scitotenv.2021.152174>.
 28. Rezaei, M., Abbasi, S., Pourmahmood, H., Oleszczuk, P., Ritsema, C., and Turner, A. (2022). Microplastics in agricultural soils from a semi-arid region and their transport by wind erosion. *Environ. Res.* 212, 113213. <https://doi.org/10.1016/j.envres.2022.113213>.
 29. Sheriff, I., Yusoff, M.S., Manan, T.S.B.A., and Koroma, M. (2023). Microplastics in manure: Sources, analytical methods, toxicodynamic, and toxicokinetic endpoints in livestock and poultry. *Environ. Adv.* 12, 100372. <https://doi.org/10.1016/j.envadv.2023.100372>.
 30. Zhang, J., Wang, X., Xue, W., Xu, L., Ding, W., Zhao, M., Liu, S., Zou, G., and Chen, Y. (2022). Microplastics pollution in soil increases dramatically with long-term application of organic composts in a wheat–maize rotation. *J. Clean. Prod.* 356, 131889. <https://doi.org/10.1016/j.jclepro.2022.131889>.
 31. Oliveri Conti, G., Rapisarda, P., and Ferrante, M. (2024). Relationship between climate change and environmental microplastics: a one health vision for the platysphere health. *One Health Adv.* 2, 17. <https://doi.org/10.1186/s44280-024-00049-9>.
 32. Haque, F., and Fan, C. (2023). Fate of microplastics under the influence of climate change. *iScience* 26, 107649. <https://doi.org/10.1016/j.isci.2023.107649>.
 33. Song, Y.K., Hong, S.H., Jang, M., Han, G.M., Jung, S.W., and Shim, W.J. (2017). Combined Effects of UV Exposure Duration and Mechanical Abrasion on Microplastic Fragmentation by Polymer Type. *Environ. Sci. Technol.* 51, 4368–4376. <https://doi.org/10.1021/acs.est.6b06155>.
 34. Lang, M., Yu, X., Liu, J., Xia, T., Wang, T., Jia, H., and Guo, X. (2020). Fenton aging significantly affects the heavy metal adsorption capacity of polystyrene microplastics. *Sci. Total Environ.* 722, 137762. <https://doi.org/10.1016/j.scitotenv.2020.137762>.
 35. Chen, L., Yu, L., Li, Y., Han, B., Zhang, J., Tao, S., and Liu, W. (2022). Spatial Distributions, Compositional Profiles, Potential Sources, and Influencing Factors of Microplastics in Soils from Different Agricultural Farmlands in China: A National Perspective. *Environ. Sci. Technol.* 56, 16964–16974. <https://doi.org/10.1021/acs.est.2c07621>.
 36. Canha, N., Jafarova, M., Grifoni, L., Gamelas, C.A., Alves, L.C., Almeida, S.M., and Loppi, S. (2023). Microplastic contamination of lettuces grown in urban vegetable gardens in Lisbon (Portugal). *Sci. Rep.* 13, 14278. <https://doi.org/10.1038/s41598-023-40840-z>.
 37. Zhang, X., Chen, Y., Li, X., Zhang, Y., Gao, W., Jiang, J., Mo, A., and He, D. (2022). Size/shape-dependent migration of microplastics in agricultural soil under simulative and natural rainfall. *Sci. Total Environ.* 815, 152507. <https://doi.org/10.1016/j.scitotenv.2021.152507>.
 38. Luo, H., Chang, L., Ju, T., and Li, Y. (2024). Factors Influencing the Vertical Migration of Microplastics up and down the Soil Profile. *ACS Omega* 9, 50064–50077. <https://doi.org/10.1021/acsomega.4c04083>.
 39. Yu, Y., Zhang, Z., Zhang, Y., Jia, H., Li, Y., and Yao, H. (2023). Abundances of agricultural microplastics and their contribution to the soil organic carbon pool in plastic film mulching fields of Xinjiang, China. *Chemosphere* 316, 137837. <https://doi.org/10.1016/j.chemosphere.2023.137837>.
 40. Liu, H., Wang, X., Shi, Q., Liu, Y., Lei, H., and Chen, Y. (2022). Microplastics in arid soils: Impact of different cropping systems (Altay, Xinjiang). *Environ. Pollut.* 303, 119162. <https://doi.org/10.1016/j.envpol.2022.119162>.
 41. IPCC (2021). Climate Change 2021: The Physical Science Basis. <https://doi.org/10.1017/9781009157896>.
 42. Li, C., Zwiers, F., Zhang, X., Li, G., Sun, Y., and Wehner, M. (2021). Changes in annual extremes of daily temperature and precipitation in CMIP6 models. *J. Clim.* 34, 3441–3460. <https://doi.org/10.1175/JCLI-D-19-1013.1>.
 43. Thrasher, B., Wang, W., Michaelis, A., Melton, F., Lee, T., and Nemani, R. (2022). NASA global daily downscaled projections, CMIP6. *Sci. Data* 9, 262. <https://doi.org/10.1038/s41597-022-01393-4>.
 44. Nwokolo, S.C., Ogbulezie, J.C., and Ushie, O.J. (2023). A multi-model ensemble-based CMIP6 assessment of future solar radiation and PV potential under various climate warming scenarios. *Optik* 285, 170956. <https://doi.org/10.1016/j.ijleo.2023.170956>.
 45. Ibarra-Berastegui, G., Sáenz, J., Ulazia, A., Sáenz-Aguirre, A., and Esnaola, G. (2023). CMIP6 projections for global offshore wind and wave energy production (2015–2100). *Sci. Rep.* 13, 18046. <https://doi.org/10.1038/s41598-023-45450-3>.
 46. Zhou, Y., Sun, Y., Liu, J., Ren, X., Zhang, Z., and Wang, Q. (2022). Effects of microplastics on humification and fungal community during cow manure composting. *Sci. Total Environ.* 803, 150029. <https://doi.org/10.1016/j.scitotenv.2021.150029>.
 47. Zhang, S., Li, Y., Chen, X., Jiang, X., Li, J., Yang, L., Yin, X., and Zhang, X. (2022). Occurrence and distribution of microplastics in organic fertilizers in China. *Sci. Total Environ.* 844, 157061. <https://doi.org/10.1016/j.scitotenv.2022.157061>.
 48. Xing, R., Chen, Z., Sun, H., Liao, H., Qin, S., Liu, W., Zhang, Y., Chen, Z., and Zhou, S. (2022). Free radicals accelerate in situ ageing of microplastics during sludge composting. *J. Hazard. Mater.* 429, 128405. <https://doi.org/10.1016/j.jhazmat.2022.128405>.
 49. Zafiu, C., Binner, E., Beigl, P., Vay, B., Ebmer, J., and Huber-Humer, M. (2023). The dynamics of macro- and microplastic quantity and size

- changes during the composting process. *Waste Manag.* 162, 18–26. <https://doi.org/10.1016/j.wasman.2023.03.002>.
50. Li, Y., Tao, L., Wang, Q., Wang, F., Li, G., and Song, M. (2023). Potential Health Impact of Microplastics: A Review of Environmental Distribution, Human Exposure, and Toxic Effects. *Environ. Health* 1, 249–257. <https://doi.org/10.1021/envhealth.3c00052>.
 51. de Ruijter, V.N., Redondo-Hasselerharm, P.E., Gouin, T., and Koelmans, A.A. (2020). Quality Criteria for Microplastic Effect Studies in the Context of Risk Assessment: A Critical Review. *Environ. Sci. Technol.* 54, 11692–11705. <https://doi.org/10.1021/acs.est.0c03057>.
 52. Weithmann, N., Möller, J.N., Löder, M.G.J., Piehl, S., Laforsch, C., and Freitag, R. (2018). Organic fertilizer as a vehicle for the entry of microplastic into the environment. *Sci. Adv.* 4, eaap8060. <https://doi.org/10.1126/sciadv.aap8060>.
 53. Steinmetz, Z., Wollmann, C., Schaefer, M., Buchmann, C., David, J., Tröger, J., Muñoz, K., Frör, O., and Schaumann, G.E. (2016). Plastic mulching in agriculture. Trading short-term agronomic benefits for long-term soil degradation? *Sci. Total Environ.* 550, 690–705. <https://doi.org/10.1016/j.scitotenv.2016.01.153>.
 54. Yuan, W., Christie-Oleza, J.A., Xu, E.G., Li, J., Zhang, H., Wang, W., Lin, L., Zhang, W., and Yang, Y. (2022). Environmental fate of microplastics in the world's third-largest river: Basin-wide investigation and microplastic community analysis. *Water Res.* 210, 118002. <https://doi.org/10.1016/j.watres.2021.118002>.
 55. Su, L., Xue, Y., Li, L., Yang, D., Kolandhasamy, P., Li, D., and Shi, H. (2016). Microplastics in Taihu Lake, China. *Environ. Pollut.* 216, 711–719. <https://doi.org/10.1016/j.envpol.2016.06.036>.
 56. Gebrechorkos, S.H., Bernhofer, C., and Hülsmann, S. (2020). Climate change impact assessment on the hydrology of a large river basin in Ethiopia using a local-scale climate modelling approach. *Sci. Total Environ.* 742, 140504. <https://doi.org/10.1016/j.scitotenv.2020.140504>.
 57. Rezaei, M., Riksen, M.J.P.M., Sirjani, E., Sameni, A., and Geissen, V. (2019). Wind erosion as a driver for transport of light density microplastics. *Sci. Total Environ.* 669, 273–281. <https://doi.org/10.1016/j.scitotenv.2019.02.382>.
 58. Zhang, W., Li, J., Liu, T., Leng, S., Yang, L., Peng, H., Jiang, S., Zhou, W., Leng, L., and Li, H. (2021). Machine learning prediction and optimization of bio-oil production from hydrothermal liquefaction of algae. *Bioresour. Technol.* 342, 126011. <https://doi.org/10.1016/j.biortech.2021.126011>.
 59. Anh, P.T.Q., Thuyet, D.Q., and Kobayashi, Y. (2022). Image classification of root-trimmed garlic using multi-label and multi-class classification with deep convolutional neural network. *Postharvest Biol. Technol.* 190, 111956. <https://doi.org/10.1016/j.postharvbio.2022.111956>.
 60. Ekanayake, I.U., Meddage, D.P.P., and Rathnayake, U. (2022). A novel approach to explain the black-box nature of machine learning in compressive strength predictions of concrete using Shapley additive explanations (SHAP). *Case Stud. Constr. Mater.* 16, e01059. <https://doi.org/10.1016/j.cscm.2022.e01059>.

STAR★METHODS

KEY RESOURCES TABLE

REAGENT or RESOURCE	SOURCE	IDENTIFIER
Deposited data		
Microplastics data	WOS and CNKI	http://www.isiknowledge.com/ and https://www.cnki.net/
Usage of mulching films and organic fertilizers	MOA	Ministry of Agriculture
Climate and topographic data, 2000–2023	CMA	https://data.cma.cn
Future scenario climate data	CMIP6	https://aims2.llnl.gov/search/cmip6/
Python	Python version 3.13.1	https://www.python.org

METHOD DETAILS

Collection of MPs data in agricultural soils

Comprehensive search was conducted using Web of Science (<http://www.isiknowledge.com/>) and CNKI (<https://www.cnki.net/>) to collect and organize peer-reviewed literature related to MPs in agricultural soils. The search keywords used were “agricultural soil” + “microplastics”, with results limited to “articles” and “reviews”. The selection criteria for the articles were as follows: (1) research focused on agricultural soils with mulching films; (2) field investigations that provided the history of mulching films (HistMF) at sampling sites; and (3) papers offering data on the morphological characteristic of MPs, specifically MPs size. From 71 articles, we extracted 230 datasets on the abundance and size of MPs in plastic-mulched agricultural soils.

Data standardization and legitimacy of integrated analysis

Data collected from the literature were generated under varying local conditions. To ensure the legitimacy and comparability of the integrated dataset for subsequent analysis, the following assumptions and standardization procedures were applied:

Methodological consistency: Only studies employing standardized methods for MPs extraction (e.g., density separation) and identification (e.g., spectroscopic techniques) were included, ensuring fundamental consistency in detection.

Unit and depth normalization: All abundance data were standardized to a uniform unit of items per kilogram (items/kg) of dry soil. Furthermore, the analysis was restricted to surface soil samples (0–30 cm depth) to mitigate biases introduced by vertical distribution variations.

Representativeness assumption: The data reported in the source studies (typically involving composite samples from multiple points within a field) were assumed to provide a representative estimate of MPs load for the given agricultural plot, making the selected representative data suitable for regional-scale modeling.

Analysis and collection of factors

We carefully selected several predictor variables to reflect the complexity of the generation and distribution of MPs in soils. These variables were categorized into two conceptual categories: anthropogenic factors and natural factors:

Anthropogenic factors. The usage of mulching films (UMF) and the application of compost are sources of MPs in farmlands. The application of compost contributes 35 billion to 2.2 trillion MPs annually to farmlands.⁵² HistMF provided insights into the fragmentation and accumulation of MPs from residual plastic mulch,⁵³ with data extracted from published literature. Using ArcGIS v.10.8 (<https://desktop.arcgis.com/>), HistMF was assigned to each county based on the precision of raster or vector maps. County-level data on annual UMF and usage of organic fertilizers (UOF) from 2000 to 2023 were sourced from the Ministry of Agriculture and Rural Affairs of China and rural statistical yearbooks, with both sources cross-verified and found to be consistent, ensuring high data reliability. Source factors include total UMF (TUMF) and total UOF (TUOF) which were calculated by multiplying the average annual usage by HistMF. Notably, mulching film in agricultural production is only used during the first half of the sowing season and only once a year, so frequency was not incorporated into the model. Furthermore, the mulching film used in Chinese agriculture is generally less than 8 μm thick, and the information of recycling rates between different regions is scarce. Additionally, the concentration of MPs in natural water sources is relatively low. For instance, the average concentration of MPs in the Yangtze River Basin is 1.27 items/L and in Taihu Lake is 11.4 items/L,^{54,55} and Chen et al. (2022) found its contribution to soil MPs pollution to be minimal.³³ Thus, differences in mulching film thickness, recycling rates, and irrigation water-induced MPs pollution were excluded from the model.

Natural factors. Climate change is closely linked to agriculture, ecosystems, socioeconomics, and human survival, and is considered one of the most pressing global issues.⁵⁶ Mechanical abrasion (e.g., wind) and UV exposure are critical factors in plastic

degradation.^{12,57} Some research has shown correlations between MPs distribution and elevation, likely due to differences in radiation intensity and human activity levels across elevations.²⁶ Moreover, plains with intensive agricultural activity and gentle slopes may contribute to the accumulation of MPs.²⁷ Therefore, climatic and topographic factors were incorporated into the machine learning model. Natural predictors included temperature (TEM), humidity (HUM), precipitation (PRE), radiation (RAD), and wind speed (WS) as climatic factors, along with slope (SL) and elevation (ELE) as topographic factors. These data were obtained from the China Meteorological Data Service Center (<https://data.cma.cn>).

Data preprocessing and machine learning modeling

We constructed a dataset consisting of 230 agricultural soil data to develop ML model, with predictor variables including HistMF, TUMF, TUOF, ELE, SL, PRE, RAD, TEM, WS, and HUM, while the target variable was either MPs abundance or MPs size. Firstly, the data were log-transformed and normalized to preserve relationships and characteristics among variables. This transformation smoothed the data by compressing the scale of the variables and reduced covariance and heteroscedasticity within the model. Additionally, we performed covariance diagnostics to check for multicollinearity and removed the redundant variable PRE (variance inflation factor, VIF = 5.29). The selected machine learning algorithms included Random Forest (RF), Extreme Gradient Boosting (XGBoost), and K-Nearest Neighbors (KNN). The dataset was stratified and randomly split into training and testing sets at a ratio of 0.8 to 0.2. These three models were benchmarked, hyperparameter tuning was performed using Bayesian optimization, and five-fold cross-validation was applied. However, since the regression model for MPs abundance and size showed suboptimal performance with R^2 values of 0.2–0.4 and relatively high MAE/RMSE, we converted it into an ordinal multiclassification model to improve prediction accuracy, and the best-performing model was selected for further interpretation and prediction.⁵⁸ For multiclassification model, evaluation metrics such as accuracy, precision, recall, and F1-score were used as standard indicators.⁵⁹

To understand the influence of features on the model, interaction features such as HistMF \times RAD and HUM \times RAD, are generated by calculating the product of feature pairs to explore the interaction effects between predictors. The SHAP (SHapley Additive exPlanations) explainable machine learning library was applied to quantify the contribution of each feature to the model's predictions, revealing the importance and correlations of features with the MPs abundance and size.⁶⁰ Partial Dependence Plots (PDP) and Individual Conditional Expectation (ICE) plots illustrate the non-linear relationships between features and the predicted outcomes, as well as to capture individual sample responses. All data preprocessing, analysis, and modeling were performed using Python version 3.13.1 (<https://www.python.org>).

Future scenario construction

For predictions of MPs abundance and size distribution up to 2050, three future scenarios were constructed: the Sustainable Development Scenario (SDS), the Business-as-Usual Scenario (BAU), and the Highly Forced Scenario (HFS). The Ministry of Agriculture and Rural Affairs of China has issued notices to promote green circular agriculture pilot programs, aiming to increase the area of organic fertilizer application by 5% by 2025. By analyzing trends in the UOF from 2000 to 2020, which show an overall upward trajectory, the UOF under all scenarios was projected based on the trends of the past two decades. Future climate data were obtained from the CMIP6 model, available at <https://esgf-node.ipsl.upmc.fr/search/cmip6-ipsi/>.

Sustainable Development Scenario (SDS). Under this scenario, due to changes in agricultural policies, increased environmental awareness, and the adoption of alternative technologies, thicker and high-strength mulching film is promoted to improve recycling rates, or fully biodegradable mulching films are used. To represent this, the annual UMF was reduced by 10%, reflecting a decrease in plastic mulch residues due to improved recycling rates or alternative technologies. A low-emission, high-mitigation climate scenario (SSP126) was selected to represent the most ideal sustainable development trajectory.

Business-as-Usual Scenario (BAU). By analyzing the trends in the UMF from 2000 to 2020, we projected its usage to 2050 under a stable climate scenario (SSP245). This scenario assumes no significant changes in agricultural practices or recycling policies and serves as a continuation of current trends.

Highly Forced Scenario (HFS). Due to agricultural intensification and low plastic recycling rates, excessive plastic waste may have long-term impacts on the sustainability of farmland ecosystems. A high-emission, low-mitigation climate scenario (SSP585) was selected to represent this scenario. This scenario is highly plausible due to rapid population growth and the absence of reliable plastic alternatives.

Expansion and prediction of MPs distribution

The expansion of MPs for 2020, 2021, 2022, and 2023 across China were generated by inputting county-level data for HistMF, TUMF, TUOF, topography, and climate variables into the XGBoost multiclassification model. Using 2020 as the baseline year, the HistMF was incremented annually. UMF and UOF, as well as climate data for 2020–2023, were derived from published datasets. The predictions for future distributions up to 2050 were also generated by inputting county-level data for HistMF, TUMF, TUOF, topography, and climate variables into the XGBoost multiclassification model under SDS, BAU and HFS scenarios, with annual data for each scenario.

Uncertainty analysis

To assess the uncertainty in the prediction results, we employed the Monte Carlo method. The input features of each sample are randomly sampled 500 times, assuming that each feature (HistMF, TUMF, TUOF, topography, and climate factors) value follows a

normal distribution with a mean equal to the original value and a standard deviation equal to 10% of the value. After performing sampling, the samples are standardized, and the model is used to predict the probability distribution for each sample. Next, we calculate the weighted average, standard deviation, and the 95% confidence interval (2.5% and 97.5% percentiles) of the predicted values to quantify the uncertainty in the predictions. Finally, we obtain the county-level prediction data and the national average prediction values along with their confidence intervals.

To identify the contribution of each variable to the uncertainty in the prediction results, we perform a One-At-a-Time (OAT) sensitivity analysis with a $\pm 10\%$ perturbation for each predictor. Specifically, for each feature, we increase and decrease its value by 10% to generate two new samples. The samples are then standardized, and the model is used to predict the changes in the results before and after perturbation. The squared difference in predictions is used as the contribution of that feature to the overall uncertainty. The contributions of all variables are then normalized, providing the relative contribution of each variable to the prediction uncertainty.

QUANTIFICATION AND STATISTICAL ANALYSIS

Statistical and machine learning analyses were carried out using Python version 3.13.1. All data preprocessing, model fitting, and evaluation were performed using established Python packages such as pandas, scikit-learn, XGBoost, PDPbox, ICEbox, shap, numpy, and scipy.